SIMULATION OF DISCRETE RANDOM FIELDS
Theoretical background

A continuous, second-order, real-valued, vector random field $\mathbf{X}(\mathbf{r},\omega)$ is specified by the expected (mean) value function

$$\bar{\mathbf{X}}(\mathbf{r}) = E\left(\mathbf{X}(\mathbf{r},\omega)\right) \tag{0.1}$$

and the correlation tensor function

$$\mathbf{K}_x(\mathbf{r}_1,\mathbf{r}_2) = E\left(\left(\mathbf{X}(\mathbf{r}_1,\omega) - \bar{\mathbf{X}}(\mathbf{r}_1)\right) \otimes \left(\mathbf{X}(\mathbf{r}_2,\omega) - \bar{\mathbf{X}}(\mathbf{r}_2)\right)\right) \tag{0.2}$$

where $E(\cdot)$ is the expectation operator, $\omega \in \Omega$ denotes an elementary event, the sign $\otimes$ denotes the tensor product, and $\mathbf{r},\mathbf{r}_1,\mathbf{r}_2 \in \Re^3$. If $\bar{\mathbf{X}}(\mathbf{r}) = \text{const}$ and

$$\mathbf{K}_x(\mathbf{r}_1,\mathbf{r}_2) = \mathbf{K}_x(\mathbf{r}_1 - \mathbf{r}_2) \tag{0.3}$$

then the field is called homogeneous, i.e. stationary in space (Adler 1981).

Using discrete methods of simulation and analysis, it is necessary to consider the random fields in the form of multidimensional random variables $\mathbf{X}$ defined on regular or irregular meshes.

Thus, the role of covariance function $\mathbf{K}_x(\mathbf{r}_1, \mathbf{r}_2)$ takes on the covariance matrix **K**, always symmetric and positively definite:

$$\mathbf{K} = E\left(\left(\mathbf{X}(\omega) - \bar{\mathbf{X}}\right)\left(\mathbf{X}(\omega) - \bar{\mathbf{X}}\right)^T\right) \tag{0.4}$$

where $\mathbf{X}(\omega)$ describes the discrete, second-order, real-valued random field and $\bar{\mathbf{X}}$ stands for the expected value vector

$$\bar{\mathbf{X}} = E\left(\mathbf{X}(\omega)\right) \tag{0.5}$$

It is also useful to define the degenerated field by the condition for the global covariance matrix **K**:

$$\det\mathbf{K} = 0 \tag{0.6}$$

The probabilistic foundation for the generation of arbitrary vector random variables has been formulated in the rejection theorem by Devroye (1986) and von Neumann (see Brandt 1998).
The main theoretical assumption of the simulation method is that the probability density function *f* of an *m*-dimensional random vector **X** is defined on a compact domain in $\Re^m$ and obeys the condition $f(\mathbf{X}) < +\infty$.
This assumption makes sense in structural mechanics.

A random point Π uniformly distributed in $\Re^{m+1}$ can be generated in the following way:

$$\Pi(\omega) = (\mathbf{x},\ u) = \begin{cases} x_i = a_i + u_i(\omega)(b_i - a_i) \\ u\ = u_{i+1}(\omega) c f_{\max} \end{cases} \tag{0.7}$$

where $(a_i,\ b_i)$, i = 1, 2,..., m are the given intervals of the reals and $u_i(\omega),\ u_{i+1}(\omega) \in U[0,1]$ are the values of independent, uniform random variables.

If $\Pi \in A$ (i.e. Π is not rejected), where $A = \{(\mathbf{x},u) : \mathbf{x} \in \Re^m,\quad 0 \le u \le cf(\mathbf{X})\}$ and $c > 0$, then the generated random variable $X_i (i = 1,2,...,m)$ is

$$X_i = a_i + u_i(b_i - a_i) \tag{0.8}$$

The direct rejection method to generate vectors **X** introduces a new dimension: a uniform, independent random variable.

In this extended $\Re^{m+1}$ space, the joint probability density defined on a suitable set, is uniform (Devroye 1986).

Fig. 3.1 presents an interpretation of the proof in the case of $m = 1$.

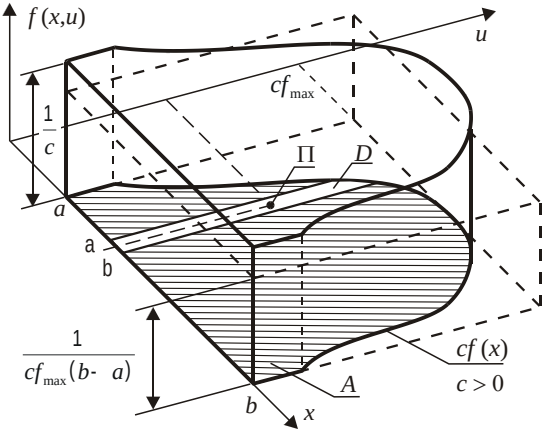

Fig. 3.1. An interpretation of Devroye theorem for $m = 1$

The random point Π is not rejected if it falls below the curve $cf(x)$ (Fig. 3.1). The probability of this event for the random variable uniformly distributed in the rectangle $cf_{\max}(b-a)$ becomes:

$$P(\Pi \in A) = \frac{\int_a^b cf(x)dx}{cf_{\max}(b-a)} = \frac{1}{f_{\max}(b-a)} \tag{0.9}$$

On the other hand, the probability for the point Π to fall below the curve $cf(x)$ (Fig. 3.1) in the interval $(\alpha,\ \beta)$ is equal

$$\frac{\int_{\alpha}^{\beta} f(x)\,dx}{f_{\max}(b-a)} \tag{0.10}$$

It follows that the ratio

$$\frac{P(\Pi \in D)}{P(\Pi \in A)} = \frac{\dfrac{\int_{\alpha}^{\beta} f(x)\,dx}{f_{\max}(b-a)}}{\dfrac{1}{f_{\max}(b-a)}} = \int_{\alpha}^{\beta} f(x)\,dx = P\left(x \in (\alpha,\ \beta)\right) \tag{0.11}$$

gives the required result.

However, the method is not effective (time inefficiency) for large values of *m*.

For that reason a method of a sequential type, by applying a propagation scheme and conditional probability distributions has been proposed.

Simulation algorithm

As the proposed algorithm concerns discretized random problems, the random fields are described by the multidimensional random variables defined at the mesh nodes.

The covariance function is represented by the symmetric and positively defined covariance matrix $\mathbf{K}(m \times m)$.

The random variable vector $\mathbf{X}(m \times 1)$ is divided into two blocks consisting of the unknown $\mathbf{X}_u(n \times 1)$ and the known $\mathbf{X}_k(p \times 1)$ elements $(n + p = m)$

$$\mathbf{X} = \begin{Bmatrix} \mathbf{X}_u \\ \mathbf{X}_k \end{Bmatrix} \begin{matrix} n \\ p \end{matrix} \tag{0.12}$$

described by a joint normal probability density $f(\mathbf{X})$

$$f(\mathbf{X}) = (\det \mathbf{K})^{-\frac{1}{2}} (2\pi)^{-\frac{m}{2}} \exp\left(-\frac{1}{2} (\mathbf{X} - \bar{\mathbf{X}})^T \mathbf{K}^{-1} (\mathbf{X} - \bar{\mathbf{X}}) \right). \tag{0.13}$$

where the covariance matrix $\mathbf{K}(m \times m)$ and the expected values vector $\bar{\mathbf{X}}(m \times 1)$ are also appropriately divided:

$$\mathbf{K} = \begin{bmatrix} \mathbf{K}_{11} & \mathbf{K}_{12} \\ \mathbf{K}_{21} & \mathbf{K}_{22} \end{bmatrix}_{p}^{n}, \qquad \bar{\mathbf{X}} = \begin{Bmatrix} \bar{\mathbf{X}}_u \\ \bar{\mathbf{X}}_k \end{Bmatrix}_{p}^{n} \tag{0.14}$$

The unknown vector $\mathbf{X}_u$ can be estimated from the following conditional distribution

$$f\left(\mathbf{X}_u / \mathbf{X}_k\right) = \frac{f\left(\mathbf{X}\right)}{f\left(\mathbf{X}_k\right)} \tag{0.15}$$

where $f(\mathbf{X}_k)$ is a normal probability density function of the known variables $\mathbf{X}_k$

$$f\left(\mathbf{X}_k\right) = \left(\det \mathbf{K}_{22}\right)^{-\frac{1}{2}} \left(2\pi\right)^{-\frac{p}{2}} \exp\left(-\frac{1}{2} \left(\mathbf{X}_k - \bar{\mathbf{X}}_k\right)^T \mathbf{K}_{22}^{-1} \left(\mathbf{X}_k - \bar{\mathbf{X}}_k\right) \right) \tag{0.16}$$

Substituting (3.13) and (3.16) into formula (3.15) yields

$$f\left(\mathbf{X}_u/\mathbf{X}_k\right)=\left(\frac{\det\mathbf{K}}{\det\mathbf{K}_{22}}\right)^{-\frac{1}{2}}\left(2\pi\right)^{-\frac{n}{2}}$$

$$\cdot\exp\left(-\frac{1}{2}\left(\begin{Bmatrix}\mathbf{X}_u\\ \mathbf{X}_k\end{Bmatrix}-\begin{Bmatrix}\bar{\mathbf{X}}_u\\ \bar{\mathbf{X}}_k\end{Bmatrix}\right)^T\left(\begin{bmatrix}\mathbf{K}_{11} & \mathbf{K}_{12}\\ \mathbf{K}_{21} & \mathbf{K}_{22}\end{bmatrix}^{-1}-\begin{bmatrix}\mathbf{0} & \mathbf{0}\\ \mathbf{0} & \mathbf{K}_{22}\end{bmatrix}^{-1}\right)\left(\begin{Bmatrix}\mathbf{X}_u\\ \mathbf{X}_k\end{Bmatrix}-\begin{Bmatrix}\bar{\mathbf{X}}_u\\ \bar{\mathbf{X}}_k\end{Bmatrix}\right)\right)$$

(0.17)

where **0** is a null matrix.

After simplification formula (3.17) can be rewritten in the following way

$$f\left(\mathbf{X}_u/\mathbf{X}_k\right)=\left(\det\mathbf{K}_c\right)^{-\frac{1}{2}}\left(2\pi\right)^{-\frac{m}{2}}\times\exp\left(-\frac{1}{2}\left(\mathbf{X}_u-\bar{\mathbf{X}}_c\right)^{\mathrm{T}}\mathbf{K}_c^{-1}\left(\mathbf{X}_u-\bar{\mathbf{X}}_c\right)\right)\quad(0.18)$$

where $\mathbf{K}_c$ and $\bar{\mathbf{X}}_c$, described as conditional covariance matrix and conditional expected value vector, can be calculated as follows:

$$\mathbf{K}_c=\mathbf{K}_{11}-\mathbf{K}_{12}\mathbf{K}_{22}^{-1}\mathbf{K}_{21}\quad(0.19)$$

$$\bar{\mathbf{X}}_c=\bar{\mathbf{X}}_u+\mathbf{K}_{12}\mathbf{K}_{22}^{-1}\left(\mathbf{X}_k-\bar{\mathbf{X}}_k\right)\quad(0.20)$$

In the case of engineering applications the random variables are usually bounded by their upper and lower limits.
For example, Young's modulus E can be estimated only by nonnegative values ($E \geq 0$), and no geometric discrepancies of any structures should cross a threshold set by relevant engineering codes.
To fulfil this requirement a formula describing the Gaussian truncated distribution is introduced

$$f_t(x) = \frac{f(x)}{P} \tag{0.21}$$

where $f(x)$ is a Gaussian density function of one-dimensional random variable X, with standard deviation σ and mean value $\bar{x}$

$$f(x) = \frac{1}{\sigma\sqrt{2\pi}} \exp\left(-\frac{(x-\bar{x})}{2\sigma^2} \right) \tag{0.22}$$

and P is the area of the Gaussian density function described by the truncation parameter s

$$P = \frac{1}{\sigma\sqrt{2\pi}} \int_{\bar{x}-s\sigma}^{\bar{x}-s\sigma} \exp\left(-\frac{(x-\bar{x})}{2\sigma^2} \right) dx \tag{0.23}$$

Putting $z = (x - \overline{x}) / \sigma$ into formula (3.23) it is easy to obtain

$$P = 2\mathrm{erf}\left(s\right) \tag{0.24}$$

where $\mathrm{erf}\,(s)$ is the error function

$$\mathrm{erf}\left(s\right) = \frac{1}{2\pi}\int_0^s \exp\left(-\frac{x^2}{2}\right)dx, \qquad \mathrm{s} \geq 0 \tag{0.25}$$

A variance of the random variable X of the Gaussian truncated distribution represents the following formula

$$\sigma_t^2 = \int_{\overline{x}-s\sigma}^{\overline{x}-s\sigma} \left(x - \overline{x}\right)^2 f_t\left(x\right)dx \tag{0.26}$$

Substituting relations (3.21) and (3.24), and performing the required integration yields

$$\sigma_t^2 = \sigma^2\left(1 - t\right) \tag{0.27}$$

where

$$t = \frac{s \cdot \exp(-s^2/2)}{\sqrt{2\pi}\ \ erf\,(s)} \tag{0.28}$$

It is easy to notice that the assumption of the truncation parameter $s=5$, usually used in the engineering applications, determines that $t \approx 0$.

Making use of the above formulas the truncated joint normal conditional distribution can be derived

$$f_t(\mathbf{X}_u/\mathbf{X}_k)=(1-t)^{-\frac{m}{2}}(\det\mathbf{K}_c)^{-\frac{1}{2}}(2\pi)^{-\frac{m}{2}}\exp\left(-\frac{1}{2(1-t)}(\mathbf{X}_u-\bar{\mathbf{X}}_c)^{\mathrm{T}}\mathbf{K}_c^{-1}(\mathbf{X}_u-\bar{\mathbf{X}}_c)\right) \tag{0.29}$$

The numerical analysis of the simulation method based on the conditional distributions (see, for example, Bielewicz et al. 1994b) has proved that the algorithm is efficient for meshes consisting of as many as 500 random values.

To improve the numerical capability of the simulation algorithm some modifications are proposed.

The changes make it possible to generate a field with a much larger number of random points.

To generate a discrete scalar random field use is made of a base scheme with random values. The scheme is placed at the nodal points of a mesh in such a way that it covers all the nodes *i*, $1 \le i \le MN$, $MN = M \times N$ (Fig. 3.2).

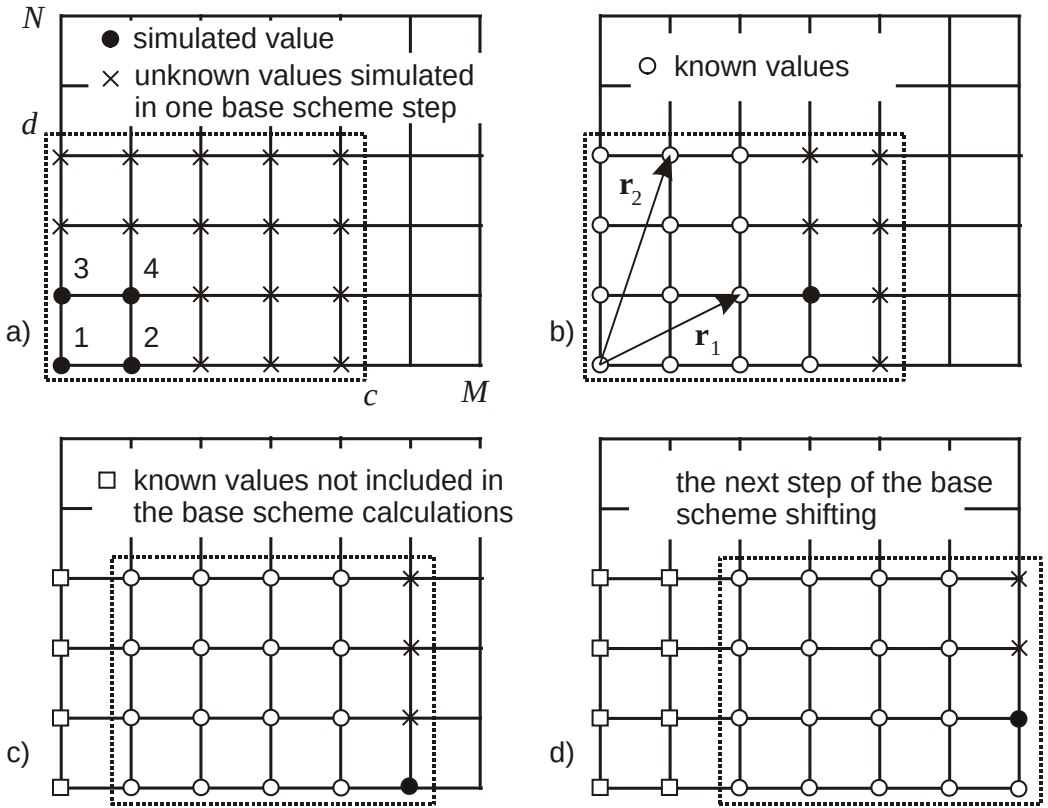

Fig. 3.2. Coverage of the field points with moving propagation scheme

The simulation process is divided into three stages.

First, the four-corner random values are generated (see Fig. 3.2a).

Next, a propagation scheme with a growing number of points covers a defined base scheme of the field mesh.

In the example shown in Fig. 3.2b the dimension of the base scheme equals $c \times d = 5 \times 5 = 20$ random values (mesh points).

In the third stage the base scheme is appropriately shifted, and the next group of unknown random values is simulated (see Fig. 3.2c and d).

The base scheme is translated so as to cover all the field nodes.

Values of the random variables at the first four points of the mesh (i = 1,..., 4) are generated using the direct rejection method (see Eq. (3.7)).

Substituting p = 0, and $m = n$ = 4 into Eqs. (3.12) and (3.14), the following random vector of unknown variables, its expected values, and the appropriate covariance matrix are obtained:

$$\mathbf{X} = \mathbf{X}_u, \qquad \bar{\mathbf{X}} = \bar{\mathbf{X}}_u, \qquad \mathbf{K} = \mathbf{K}_{11} \tag{0.30}$$

The truncated density function of $\mathbf{X}$ is used in the generation

$$f_t(\mathbf{X}) = (1-t)^{-2} (\det \mathbf{K})^{-\frac{1}{2}} (2\pi)^{-2} \exp\left(-\frac{1}{2(1-t)} (\mathbf{X}-\bar{\mathbf{X}})^T \mathbf{K}^{-1} (\mathbf{X}-\bar{\mathbf{X}}) \right) \qquad (0.31)$$

where *t* is the assumed truncated parameter whose value is assumed according to the generated field properties.

The generation process consists of the following steps:

1. Generation of random vector $\mathbf{X}_u(4\times1)$ with the components:

   $$X_i = a_i + (b_i - a_i) u_i, \quad i = 1,...,4, \qquad (0.32)$$

   where u_i are the random variables uniformly distributed in the interval [0,1], and $(a_i,\ b_i)$, $i = 1, 2, \ldots, m$ are intervals of the reals.
2. Generation of random variable *u* from the interval [0,1] and definition of the value

   $$f_{\max} = u\Phi, \qquad \Phi = (1-t)^{-2} (\det \mathbf{K})^{-1/2} (2\pi)^2 \qquad (0.33)$$

   where $\mathbf{K}(4\times4)$ is the local covariance matrix and $\mathbf{\Phi}$ bounds the conditional density function.

3. Calculation of the density function $f(\mathbf{X}_u)$

$$f(\mathbf{X}_u) = \Phi \exp\left(-\frac{1}{2(1-t)} J(\mathbf{X}_u) \right) \tag{0.34}$$

where

$$J(\mathbf{X}_u) = \left(\mathbf{X}_u - \bar{\mathbf{X}}_u\right)^T \mathbf{K}^{-1} \left(\mathbf{X}_u - \bar{\mathbf{X}}_u\right) \tag{0.35}$$

4. Checking the condition

$$f_{\max} \le f(\mathbf{X}_u) \tag{0.36}$$

If this condition holds, vector $\mathbf{X}_u(4\times 1)$ is accepted and if not, the calculations are repeated.

For any point of the base mesh "i", $5 \le i \le (c \times d)$, where $(c \times d)$ denotes the dimension of the base scheme (see Fig. 3.2a) the only unknown random value is X_i, whereas other random variables $X_1 \div X_{i-1}$ are known.

In the calculations it is necessary to make the following substitutions in formulas (3.12) and (3.14): $m = i$, $n = 1$, $p = i - 1$. It is easy to notice that the problem is reduced to one-dimensional ($\mathbf{K}_c \equiv K_c$, $\bar{\mathbf{X}}_c \equiv \bar{X}_c$).

It makes the generation easier and relatively fast.

The calculations include the following operations:

1. Determination of the local covariance matrix $\mathbf{K}(i \times i)$, and determination of the known part of the random vector $\mathbf{X}_k((i-1)\times 1)$, as well as the expected values vector $\overline{\mathbf{X}}(i \times 1)$, according to formulas (3.12) and (3.14), respectively.
2. Calculation of the conditional variance K_c and the mean $\overline{X}_c$ on the basis of equations (3.19) and (3.20):

$$K_c = K_{11} - \mathbf{K}_{12}\mathbf{K}_{22}^{-1}\mathbf{K}_{21} \tag{0.37}$$

$$\overline{X}_c = \overline{X}_u + \mathbf{K}_{12}\mathbf{K}_{22}^{-1}\left(\mathbf{X}_k - \overline{\mathbf{X}}_k\right) \tag{0.38}$$

3. Generation of random variable X_i:

$$X_i = a_i + \left(b_i - a_i\right)u_i \tag{0.39}$$

4. Generation of the independent random variable *u* from interval [0,1] and definition of the value

$$f_{\max} = u\Phi, \qquad \Phi = \left(1-t\right)^{-(i-1)/2}\left(2\pi K_c\right)^{-1/2} \tag{0.40}$$

5. Calculation of the density function $f(X_i)$

$$f(X_i) = \Phi \exp\left(-\frac{1}{2(1-t)} J(X_i) \right) \tag{0.41}$$

where

$$J(X_i) = \frac{\left(X_i - \bar{X}_c\right)^2}{K_c} \tag{0.42}$$

6. Checking the condition

$$f_{\max} \le f(X_i) \tag{0.43}$$

If this condition holds, the random value X_i is accepted and if not, the calculation returns to point three.

Intervals (a_i, b_i) are fixed for every node. The assumed standard deviation σ_i at the node i is connected with the interval by equation

$$\left(\int_{a_i}^{b_i} \left(x_i - \bar{x}_i\right)^2 f(x_i)\, dx_i \right)^{1/2} = \sigma_i \tag{0.44}$$

The proposed method of covering the random field with the defined base schemes makes it possible to analyse the meshes with a large number of points. The maximum dimension of the covariance matrix **K** is defined by the base scheme size.

The numerical analysis leads to the conclusion that 400 mesh points are an optimal base dimension.

The symmetry of the matrix **K** (see Eq. (3.14)) significantly reduces the calculations.

It should be pointed out that according to the proposed algorithm the single random value is calculated on the assumption that the random values only in the close neighbourhood (the base mesh) are known.

The specific way of covering the random field has a significant effect on the accuracy of the calculations.

In strongly correlated fields the convergence of the simulation process can lead to considerable discrepancies.

This procedure can be used for simulation of arbitrary planes or three-dimensional random fields. The meshes can also be irregular.

Accuracy analysis of simulated random fields

To examine the correctness of the proposed method the following scalar, zero-mean value correlation functions have been considered in numerical examples:

– —White noise field $N(\mathbf{r},\omega)$

$$K_N(\mathbf{r}_1,\mathbf{r}_2)=\sigma^2\delta(\mathbf{r}_1-\mathbf{r}_2) \tag{0.45}$$

– —the Wiener field (non-homogeneous) $W(\mathbf{r},\omega)$

$$K_W(\mathbf{r}_1,\mathbf{r}_2)=\alpha^2\min(r_{1x},r_{2x})\times\min(r_{1y},r_{2y})\times\min(r_{1z},r_{2z}) \tag{0.46}$$

– —the Brown field (locally non-deterministic)

$$K_B(\mathbf{r}_1,\mathbf{r}_2)=0.5\beta^2\left(\|\mathbf{r}_1\|+\|\mathbf{r}_2\|-\|\mathbf{r}_1-\mathbf{r}_2\|\right) \tag{0.47}$$

– —Homogeneous (Shinozuka) field $S(\mathbf{r},\omega)$ (Shinozuka 1987a).

$$K_S(\mathbf{r}_1,\mathbf{r}_2)=\alpha_0^2\exp\left(-\alpha_1^2(r_{1x}-r_{2x})^2-\alpha_2^2(r_{1y}-r_{2y})^2-\alpha_3^2(r_{1z}-r_{2z})^2\right) \tag{0.48}$$

where $\mathbf{r}\in\Re_+^2$ is the position vector (Fig. 3.2a) and α, β, α_0, α_1, α_2, α_3, ρ are arbitrary positive constants, $\|\cdot\|$ denotes the standard Euclidean norm (distance) and δ stands for the Dirac delta.

It should be mentioned that the developed computer program can be applied to generate any plane or spatial fields.

Statistical formulas give the estimators of the mean value $\hat{\mathbf{w}}$ and the global covariance matrix $\hat{\mathbf{K}}$ of the generated set of realizations:

$$\hat{\mathbf{w}} = \frac{1}{NR}\sum_{i=1}^{NR}\mathbf{w}_i$$
$$\hat{\mathbf{K}} = \frac{1}{NR-1}\sum_{i=1}^{NR}(\mathbf{w}_i - \hat{\mathbf{w}})(\mathbf{w}_i - \hat{\mathbf{w}})^{\mathrm{T}} \qquad (0.49)$$

where $\mathbf{w}_i$ is the random vector and NR is the number of realizations in the set. The following definition of the global error G_{er} allows to compare the estimator of the covariance matrix $\hat{\mathbf{K}}$ with the theoretical one $\mathbf{K}$:

$$G_{er} = \frac{\left(\|\mathbf{K}\| - \|\hat{\mathbf{K}}\|\right)}{\left(\|\mathbf{K}\|\right)} \times 100\% \qquad (0.50)$$

where $\|\mathbf{K}\| = \sqrt{tr(\mathbf{K}^2)}$ is the Euclidean norm.

The error of variances V_{er} and the local error L_{er} of a single element of covariance matrix can also be used:

$$V_{er} = \sum_{i=1}^{MN} \frac{\left(k_{ii} - \hat{k}_{ii}\right)}{k_{ii}} \times 100\%, \qquad L_{er} = \frac{\max\left(k_{ij} - \hat{k}_{ij}\right)}{\sqrt{k_{ii} k_{jj}}} \times 100\% \tag{0.51}$$

where k_{ij} and $\hat{k}_{ij}$ denote the element of the theoretical covariance matrix and its estimator respectively.

The mesh dimensions of the simulated fields described by Equations (3.45) $\div$ (3.48) are the same as the size of the engineering examples calculated in the next sections.

In this way the correctness analysis is strictly related to the problems which are solved in the present work.

Two different meshes for the generation of the random fields have been selected.

First, a plane square 11×11 mesh (121 nodes) is chosen. In all cases $r_x, r_y \in <1.0, 11.0>$ (Fig. 3.2).

The values of the positive constant (see formula (3.45) ÷ (3.48)) are assumed to be: $\alpha = 1.0$ (the Wiener field), $\beta = 1.0$ (the Brown field), $\alpha_0^2 = 1.0$, $\alpha_1 = \alpha_2 = 0.25$ (homogeneous field), and the parameter *s* (see the formula (3.28)) equals *s* = 5.

For these 11 × 11 meshes the generation processes can be performed using a single base scheme (see Fig. 3.2 a and b).

To check if the errors of the fields generations decrease with the number of calculated realizations the following tests are performed.

For each field (3.45) ÷ (3.48) one hundred independent trials (*NT* = 100) are carried out.

Ten thousand realizations (*NR* = 10000) are generated in a single trial.

The expected value of global errors of covariance matrix $E(G_{er})$ (Eq. (3.50)), error of variances $E(V_{er})$, and single element error $E(L_{er})$ (Eqs (3.51)) are calculated every 100th realizations using the following formulas:

$$E\left(G_{er}\right)=\frac{1}{NT}\sum_{i=1}^{NT}\left(G_{er}\right)_i$$

$$E\left(V_{er}\right)=\frac{1}{NT}\sum_{i=1}^{NT}\left(V_{er}\right)_i \qquad (0.52)$$

$$E\left(L_{er}\right)=\frac{1}{NT}\sum_{i=1}^{NT}\left(L_{er}\right)_i$$

Also the variances of these errors are introduced:

$$D^2\left(G_{er}\right)=\frac{1}{NT-1}\sum_{i=1}^{NT}\left(\left(G_{er}\right)_i-E\left(G_{er}\right)\right)^2$$

$$D^2\left(V_{er}\right)=\frac{1}{NT-1}\sum_{i=1}^{NT}\left(\left(V_{er}\right)_i-E\left(V_{er}\right)\right)^2 \qquad (0.53)$$

$$D^2\left(L_{er}\right)=\frac{1}{NT-1}\sum_{i=1}^{NT}\left(\left(L_{er}\right)_i-E\left(L_{er}\right)\right)^2$$

The results are presented in Fig. 3.3 ÷ Fig. 3.6. The plotted functions of the calculated mean errors and the standard deviations are different in each case of the random fields.

The same characteristic features are common, for example:

- all the calculated error functions are visibly decreasing, in the most cases very fast,
- the maximal errors of a single element computation scatter much more in comparison with other estimators,
- the errors of the variance calculation are always smaller than other estimators.

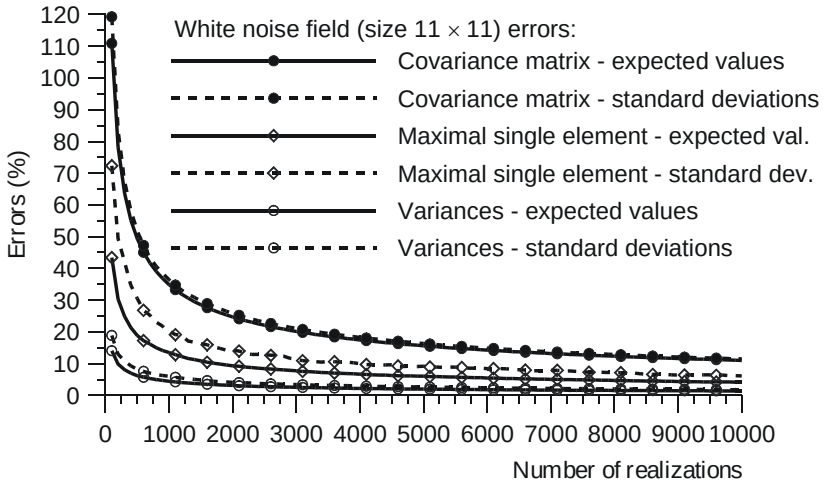

Fig. 3.3. Error analysis of white noise field generations (size 11 × 11)

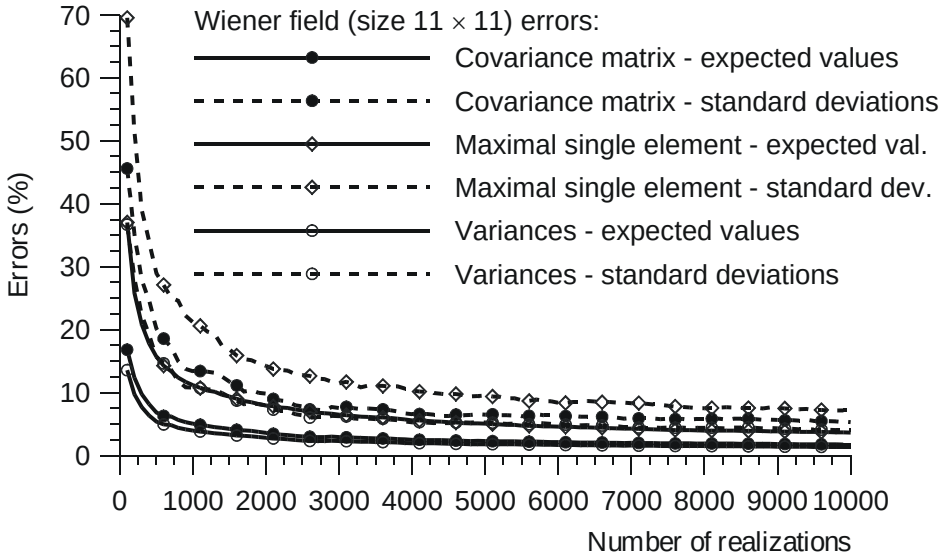

Fig. 3.4. Error analysis of the Wiener field generations (size 11 × 11)

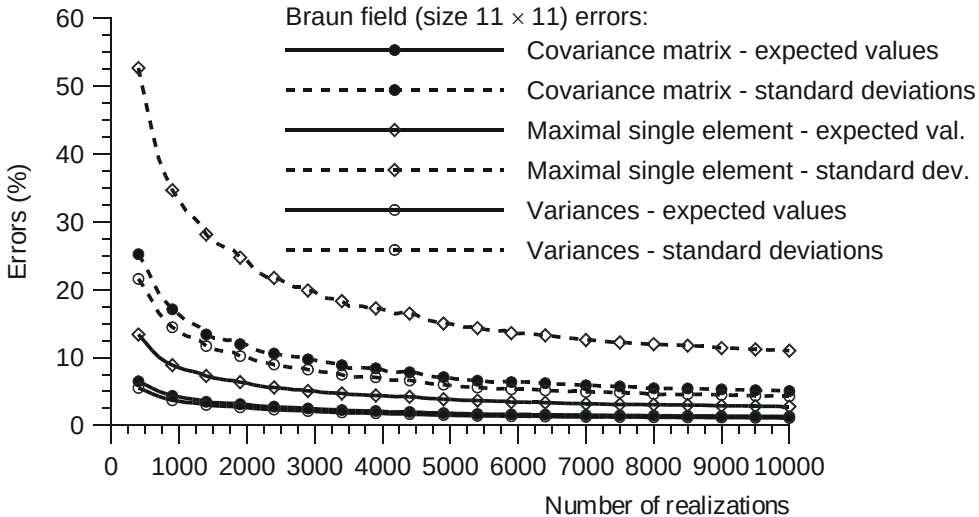

Fig. 3.5. Error analysis of the Braun field generations (size 11 × 11)

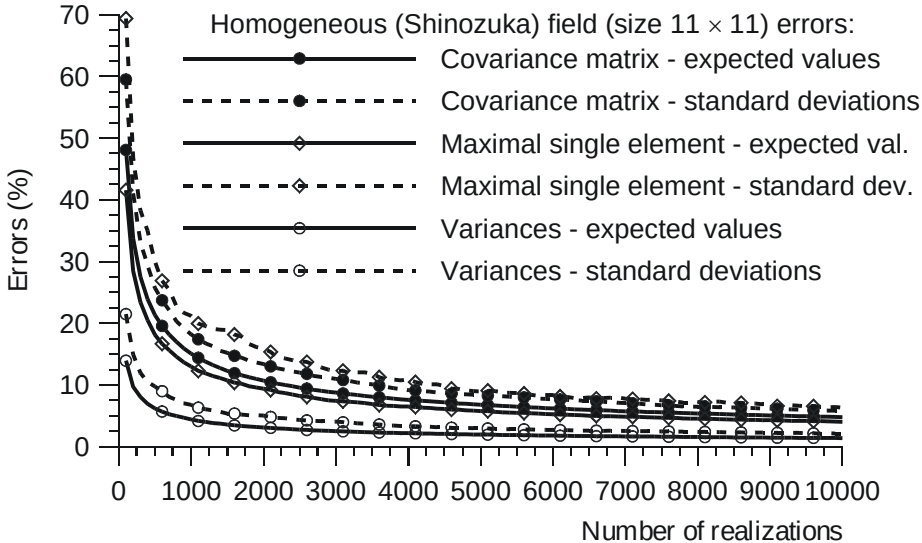

Fig. 3.6. Error analysis of homogeneous field generations (size 11 × 11)

In general it can be asserted that most crucial global errors of the covariance matrix $E(G_{er})$ start to be less than 10% from approximately 2000 ÷ 3000 realizations (the white field is an exception).

Also, from this number of realizations the errors stabilization is noticeable. For this reason it should be assumed that at least 2000 realizations is needed in order to reproduce the prescribed correlation functions properly.

The exact number of simulation should be checked in each case individually.

Additionally, graphical comparisons between the theoretical covariance matrices $\mathbf{K}$ and the estimators $\hat{\mathbf{K}}$ (Eq. (3.49)) for the four random fields (3.45) ÷ (3.48) are created, and the results are presented in Fig. 3.7.

In each case the lower triangle represents the generated field while the upper triangle the theoretical one.

The figures allow for a visual check of the correctness of the simulated fields.

Moreover, one can note that the selected correlation functions (3.45) ÷ (3.48) are very different, and because of that the verifying analysis has a comprehensive meaning.

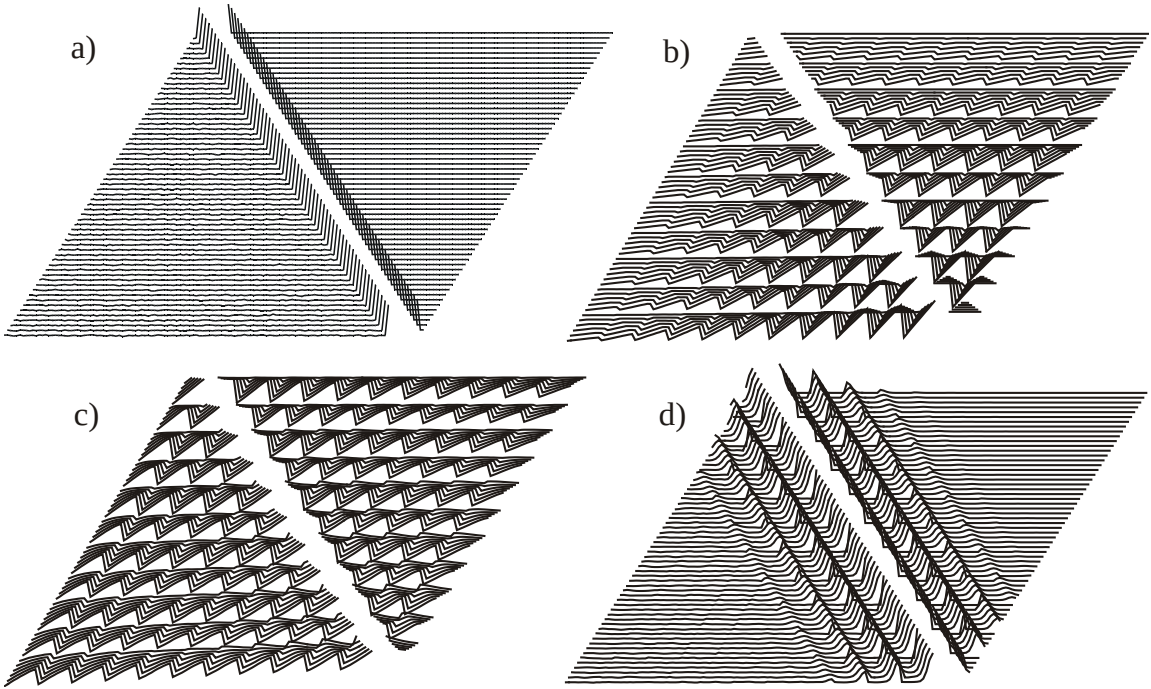

Fig. 3.7. Comparison of the target covariance matrices (upper triangles) with the simulated matrices (lower triangles): a) White noise field, b) the Wiener field, c) the Brown field, d) homogeneous field

Comparing the graphical presentations of the simulated fields (Fig. 3.7) and their errors function (Fig. 3.3 ÷ Fig. 3.6) an additional conclusion can be formulated.

For example, the global covariance matrix errors is greater in the case of the white noise field (Fig. 3.3) and the homogeneous field (Fig. 3.6).

Analysing the fields graphical presentation in Fig. 3.7a and d, it can be stated that a great part of the theoretical covariance matrix values equal zero.

As the matrix element estimators have non-zero values (see Fig. 3.7) the calculated errors are remarkably high.

Some examples of the simulated single realizations are presented in Fig. 3.8.

Also the graphical presentation of these realizations allows for specifying the type of the random field analysed.

For example, observing the results presented in Fig. 3.7 and Fig. 3.8 one can find out if the field is a correlated one.

Next, a much bigger mesh is analysed.

A plane discrete field, $16 \times 308 = 4928$ nodes has been chosen.

The same dimension field (but described by different correlation function) is used in Chapter 7 to analyse a petrol tank with initial geometric imperfection.

Only one homogeneous (Shinozuka) correlation function (3.48) has been used in the generation process.

This field seems to be an appropriate description of many two- and three-dimensional engineering problems, illustrating geometric imperfections of steel plates and shells or spatial variability of material parameters of soil, for example.

The same values of the positive constant are assumed ($\alpha_0^2 = 1.0$, $\alpha_1 = \alpha_2 = 0.25$) as in the previous calculation.

The size of the field determines the use of the shifted scheme method of generation (see Fig. 3.2). 16 × 16 points scheme has been chosen.

It is easy to note that to cover all the random field points the scheme must be shifted 308 – 16 = 292 times.

Only one series of calculations has been performed and the results are presented in Fig. 3.9.

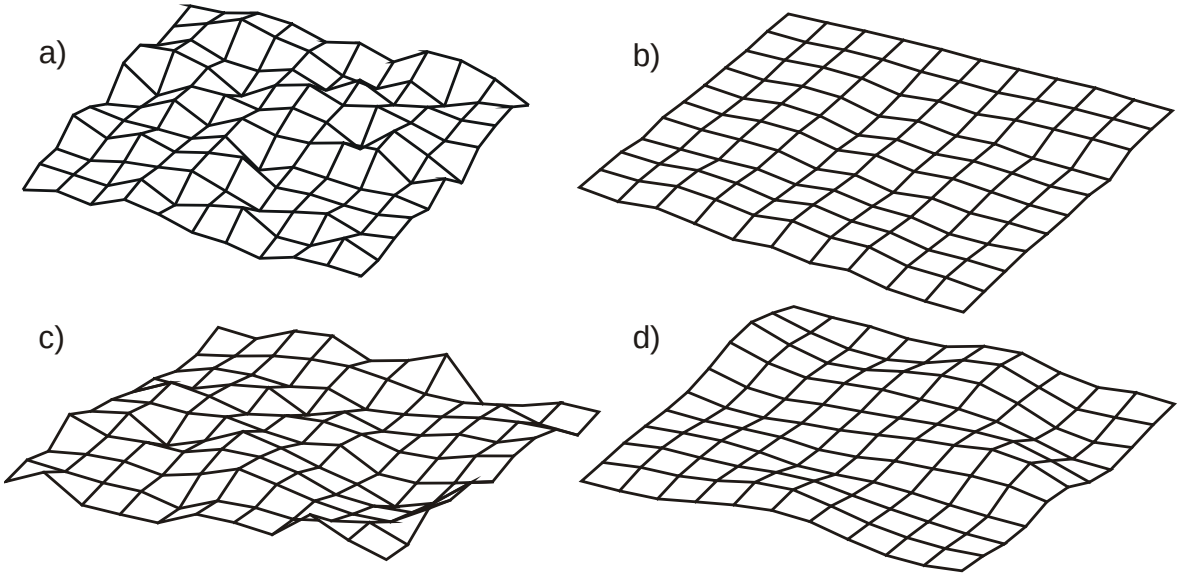

Fig. 3.8. Examples of realizations of the simulated fields:
a) White noise,
b) the Wiener field,
c) the Brown field,
d) homogeneous field

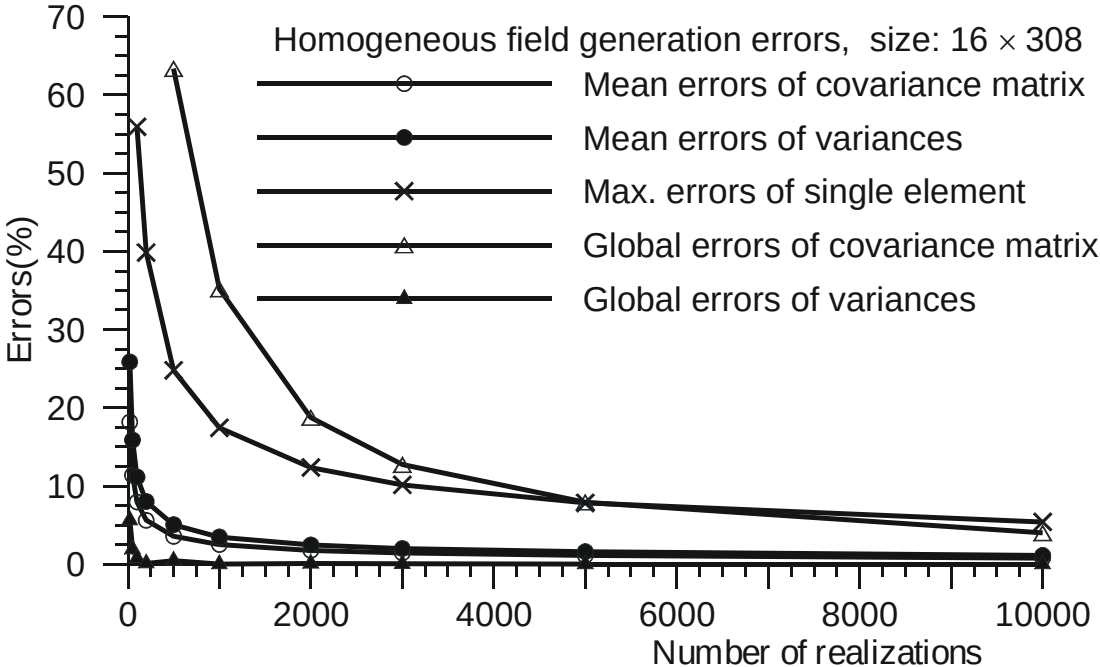

Fig. 3.9. Error analysis of Shinozuka (homogeneous) field generations (size 16 × 308)

Compared to the previous convergence analysis a standard mean error of covariance matrix and variances has also been calculated (see Fig. 3.9).

The obtained global covariance error is bigger in comparison with the 11×11 field generation (Fig. 3.6).

Nevertheless, the results proved that the generation of real engineering fields is possible and accurate.

To prove the correctness of the proposed generation method an additional test for the Brown and Wiener fields proposed by Walukiewicz has been performed (see Walukiewicz et al. 1995).

As in the first step of the analysis one hundred independent trials for 11×11 fields have been carried out.

From the estimation theory (Krishnaiah, 1994) it is known that theoretical distributions of estimators for some characteristics of the multidimensional normal random variables can be derived on the basis of the Wishart (gamma) distribution.

In the following the theoretical distributions of variances and covariances (local characteristic), as well as the distributions of the determinants of the covariance matrices (global characteristic) are calculated.

To start with, the probability distribution for the estimator of the covariance matrix $\hat{\mathbf{K}}$ was derived. Since $\hat{\mathbf{K}}$ is a symmetric matrix of dimension ($m \times m$), the following joint probability distribution is defined in space $\Re^{m(m+1)/2}$

$$f\left(\hat{\mathbf{K}}(NR),\mathbf{K}\right) = C(NR,m)(\mathbf{K})^{-\frac{NR}{2}}\left(\hat{\mathbf{K}}\right)^{\frac{NR-m-1}{2}} \times \exp\left(-\frac{NR}{2}\mathrm{tr}\left(\mathbf{K}^{-1}\hat{\mathbf{K}}\right)\right) \quad (0.54)$$

where the constant $C(NR,m)$ is calculated from the normalization condition:

$$C(NR,m) = \left(NR^{-\frac{NR\times m}{2}} 2^{\frac{NR\times m}{2}} \pi^{m(m-1)} \prod_{j=1}^{m} \Gamma\left(\frac{NR+1-j}{2}\right)\right)^{-1} \quad (0.55)$$

The condition $NR > m-1$ must be fulfilled for positively defined $\hat{\mathbf{K}}$ (almost surely).

Function Γ is defined for positive real arguments or for some natural arguments as:

$$\Gamma(y) = \int_0^{\infty} x^{y-1} e^{-x} dx \tag{0.56}$$

or $$\Gamma(NR) = (NR-1)! \tag{0.57}$$

If matrix $\hat{\mathbf{K}}$ is not positively defined then the probability distribution vanishes.

From formula (3.54) one obtains the probability distribution for a single variance estimator $\hat{\sigma}^2$ $(m=1)$:

$$f\left(\hat{\sigma}^2\left(NR,\sigma^2\right)\right) = \frac{\left(\sigma^2\right)^{-\frac{NR}{2}} NR^{\frac{NR}{2}} \left(\hat{\sigma}^2\right)^{\frac{NR-2}{2}}}{2^{\frac{NR}{2}}\Gamma\left(\frac{NR}{2}\right)} \times \exp\left(-\frac{NR}{2}\frac{\hat{\sigma}^2}{\sigma^2}\right) \tag{0.58}$$

where σ^2 is the theoretical variance of the simulated field at a point.

The histograms of the variances of the Wiener and the Brown fields are presented in Fig. 3.10 and Fig. 3.11.

These results show a very good agreement with the theoretical (Wishart) distribution.

Next, the first two moments of the estimated covariance matrix determinant $(\hat{\mathbf{K}})$ are calculated

$$E\left((\hat{\mathbf{K}})\right) = \frac{1}{NR^m}\left[(NR-1)(NR-2)...(NR-m)\right] \ (\mathbf{K})$$
$$E\left((\hat{\mathbf{K}})^2\right) = \left(\prod_{j=1}^{m}\left(1+\frac{1-j}{NR}\right)\left(1+\frac{3-j}{NR}\right)\right) \ (\mathbf{K})^2 \qquad (0.59)$$

For the Wiener field and the Braun fields the sampled (100 samples) and the theoretical moments (formulas (3.59)) are calculated, as the functions of the number of realizations.

These moments are presented in Fig. 3.12. One can observe a striking agreement of the estimated (generated) moments with the theoretical predictions.

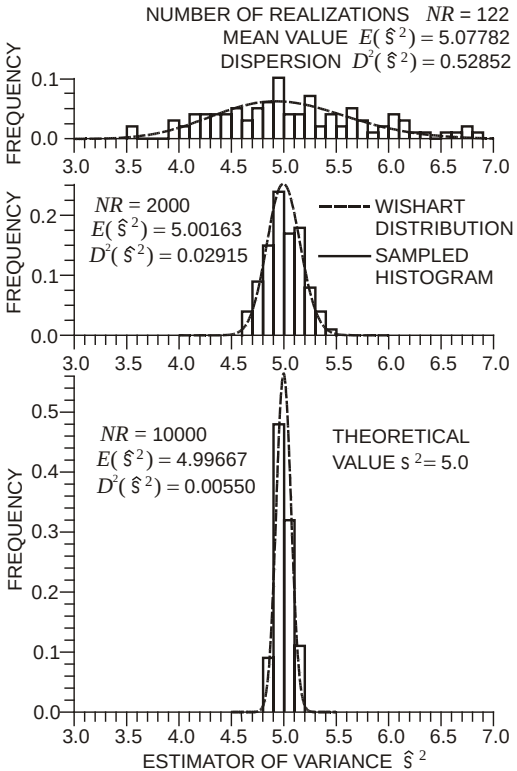

Fig. 3.10. Distribution of the Brown field sampled variances versus the Wishart distribution

Further investigation based on Shannon's measure of information (see, for example, Aczél and Daróczy 1975, Sobczyk 1973, or Sobczyk and Spencer 1996) has been performed by Walukiewicz (1997a and 1997b).

A statistical analysis of the simulated various homogeneous and nonhomogeneous, second-order random fields proved a high accuracy and some universality of the proposed method of simulation.

The method will be especially useful in the simulation-based approach.

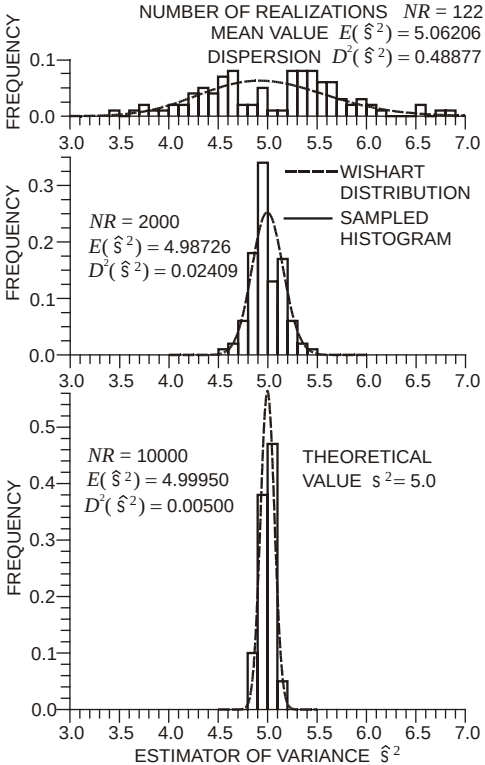

Fig. 3.11. Distribution of the Wiener field sampled variances versus the Wishart distribution

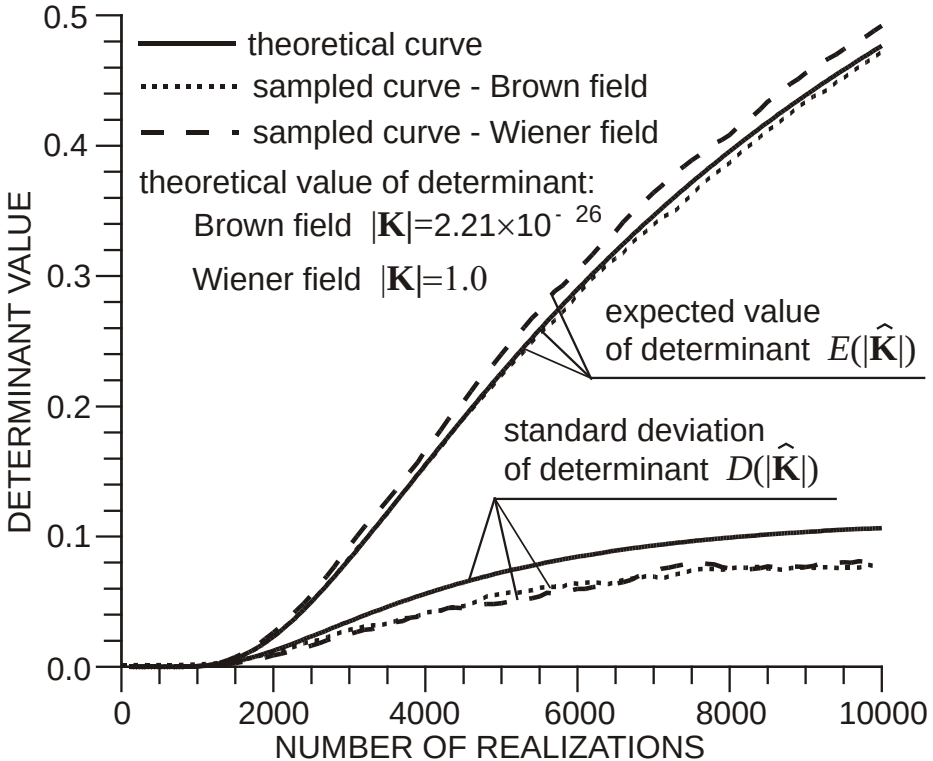

Fig. 3.12. Moments of sampled covariance matrix determinants versus theoretical moments